*Inorg. Chem.* **2008**, *47*, 209–218


# Helicates, Boxes, and Polymers from Simple Pyridine-Alcohol Ligands: the Impact of the Identity of the Transition Metal Ion

**Shane G. Telfer,*,† Nyree D. Parker,† Reiko Kuroda,‡,§ Takunori Harada,‡ Julie Lefebvre,£ and Daniel B. Leznoff£**

*MacDiarmid Institute for Advanced Materials and Nanotechnology, Institute of Fundamental Sciences, Massey University, Private Bag 11 222, Palmerston North, New Zealand, JST ERATO-SORST Kuroda Chiromorphology Team, 4-7-6 Komaba, Meguro-ku, Tokyo, 153-0041, Japan, Department of Life Sciences, Graduate School of Arts and Sciences, University of Tokyo, Komaba, Meguro-ku, Tokyo, 153-8902, Japan, and Department of Chemistry, Simon Fraser University, 8888 University Drive, Burnaby, British Columbia, Canada V5A 1S6*

Received September 7, 2007

The coordination chemistry of 6-methylpyridine-2-methanol (**1**) and enantiopure (*R*)-1-(6-methylpyridin-2-yl)ethanol (**2**) with a range of divalent first-row transition metal salts has been investigated in an effort to determine whether hydrogen-bonded helicates will form, as observed for cobalt(II) salts. Hydrogen-bonded helicates, $[Cu_2(\mathbf{1})_2(\mathbf{1}\text{-H})_2X_2]$ (X = Cl, Br), were only observed upon combining **1** with $CuCl_2$ and $CuBr_2$ in MeOH solution. Other metal salts led to alternative products, viz. $Cu(ClO_4)_2$ in the presence of base gives $[Cu_2(\mathbf{1})_2(\mathbf{1}\text{-H})_2](ClO_4)_2$, $ZnCl_2$ and $ZnBr_2$ give the 1-D helical coordination polymers $[Zn(\mathbf{1}\text{-H})Cl]_\infty$ and $[Zn(\mathbf{1}\text{-H})Br]_\infty$, a mixture of $NiCl_2$ and $Ni(OAc)_2$ produces the $[Ni_4(\mathbf{1}\text{–H})_4Cl_2(OAc)_2(MeOH)_2]$ cubane, $NiCl_2$ leads to the $[Ni_4(\mathbf{1}\text{–H})_4Cl_4(MeOH)_4]$ cubane, while $MnCl_2$ gives the known cubane $[Mn_4(\mathbf{1}\text{–H})_6Cl_4]$. The reaction of **2** with $CuCl_2$ produces the mononuclear complex $\Lambda$-$[Cu(\mathbf{2})_2Cl]Cl$, while reaction with $CuBr_2$ leads to a dimer, $\Lambda,\Lambda$-$[Cu_2(\mathbf{2})_3(\mathbf{2}\text{-H})Br_2]Br$, which is held together by a single hydrogen bond between the monomeric subunits. The solid-state CD spectra of these latter complexes were recorded and found to be very similar. The temperature-dependent magnetic behavior of $[Cu_2(\mathbf{1})_2(\mathbf{1}\text{-H})_2X_2]$ (X = Cl, Br), $[Cu_2(\mathbf{1})_2(\mathbf{1}\text{-H})_2](ClO_4)_2$, $[Cu_2(\mathbf{2})_3(\mathbf{2}\text{-H})Br_2]Br$, and $[Ni_4(\mathbf{1}\text{–H})_4Cl_2(OAc)_2(MeOH)_2]$ was investigated. Weak antiferromagnetic coupling between the copper(II) centers is mediated by the hydrogen bonds in the $[Cu_2(\mathbf{1})_2(\mathbf{1}\text{-H})_2X_2]$ (X = Cl, Br) complexes.

## Introduction

One domain of coordination chemistry that has flourished in recent years is the synthesis of complex supramolecular architectures via self-assembly processes involving metal salts and organic ligands. Most often these ligands must be synthesized by conventional procedures, and this often represents the most time-consuming step in the synthesis of any given assembly. Circumvention or simplification of this step can lead to considerable gains in efficiency, and may greatly facilitate studies that probe the effect of changes in the ligand structure, metal ion, and/or reaction conditions on the outcome of the self-assembly process. We[1−3] and others[4,5] have been interested in methods of improving the overall efficiency of the synthesis of metallo-supramolecular architectures by using ligands that are themselves built up using noncovalent interactions. As shown in Scheme 1, we have focused on transition metal helicates that feature ligand strands that are built up using hydrogen bonds. These strands are constructed as part of the overall self-assembly process, which is a simple "one-pot" procedure involving the combination of pyridine-alcohol ligands such as 6-meth-

* To whom correspondence should be addressed. E-mail: s.telfer@massey.ac.nz.
† Massey University.
‡ JST ERATO-SORST Kuroda Chiromorphology Team.
§ University of Tokyo.
£ Simon Fraser University.

(1) Telfer, S. G.; Sato, T.; Kuroda, R. *Angew. Chem., Int. Ed.* **2004**, *43*, 581−584.
(2) Telfer, S. G.; Kuroda, R. *Chem. Eur. J.* **2005**, *11*, 57−68.
(3) Telfer, S. G.; Kuroda, R.; Lefebvre, J.; Leznoff, D. B. *Inorg. Chem.* **2006**, *45*, 4592−4601.
(4) Lam, M. H. W.; Cheung, S. T. C.; Fung, K.-M.; Wong, W.-T. *Inorg. Chem.* **1997**, *36*, 4618−4619.
(5) Sun, X.; Johnson, D. W.; Caulder, D. L.; Raymond, K. N.; Wong, E. H. *J. Am. Chem. Soc.* **2001**, *123*, 2752−2763.

10.1021/ic701757e CCC: $40.75 
Published on Web 12/11/2007

**Scheme 1.** Formation of Hydrogen-Bonded Helicates, $[Co_2(\mathbf{1})_2(\mathbf{1}\text{-}H)_2X_2]$, From the Reaction of Ligands **1** and **2** with $CoX_2$ Salts

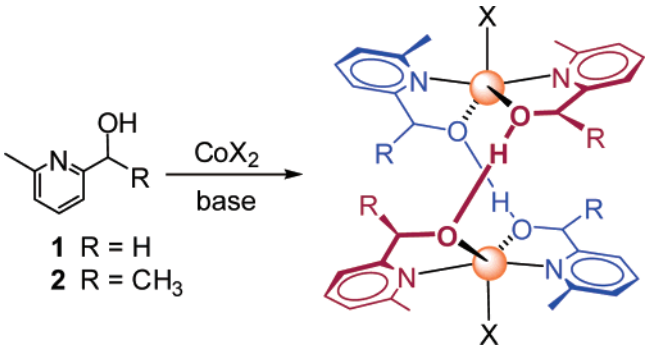


ylpyridine-2-methanol (**1**) and 1-(6-methylpyridin-2-yl)-ethanol (**2**) with various $CoX_2$ salts. These assemblies, termed hydrogen-bonded helicates, have been characterized in both the solid state and solution,[2] their magnetic behavior has been investigated,[3] and a systematic investigation into the roles of the counteranion, ligand structure, the solvent and added base on the self-assembly process has been carried out.[3]

We were interested to see whether similar structures would form if other divalent, first-row transition metal salts were combined with **1** and (*R*)-**2** under similar reaction conditions. As detailed in this report, we have focused on manganese(II), nickel(II), copper(II), and zinc(II) salts. We have found that only the copper(II) salts yield hydrogen-bonded helicates under the reaction conditions used to produce the cobalt(II) helicates. Other metal ions lead to a variety of structural motifs including dimers, cubanes, and coordination polymers. This work highlights the remarkable versatility of the coordination and supramolecular chemistry of simple pyridine-alcohol ligands.

Apart from our investigations into the formation of hydrogen-bonded helicates from **1**, the coordination chemistry of this ligand has only occasionally been studied. The thermodynamic stability constants of the $[Cu(\mathbf{1})]^{2+}$ and $[Cu(\mathbf{1})_2]^{2+}$ complexes have been determined potentiometrically,[6] and the $[Cu(\mathbf{1}-H)(OAc)]_2$ dimer has been structurally characterized.[7] Also, Zn(II)−thiolate complexes of this ligand have been used as structural models of alcoholdehydrogenase,[8] and the magnetic behavior of polynuclear manganese(II) and iron(III) complexes that contain **1** has been investigated.[9,10]

In contrast, the parent ligand, pyridine-2-methanol, has been well studied. This ligand exhibits a rich coordination chemistry, forming a diverse range of mononuclear,[11,12] dinuclear,[13] polynuclear complexes,[14−16] and polymeric structures.[17] Although this ligand does not form hydrogen-bonded helicates akin to ligand **1**,[2] certain of its complexes[14−16] display cubane-like structures that closely resemble some of the complexes formed by ligand **1**, as outlined in the present report.

## Results and Discussion

**Conditions Previously Employed for the Synthesis of Cobalt(II) Helicates.** We have previously observed that the reaction of **1** with $CoX_2$ salts (X = e.g., $Cl^-$, $Br^-$, $NO_3^-$, $SCN^-$) produces hydrogen-bonded helicates, $[Co_2(\mathbf{1})_2(\mathbf{1}\text{-}H)_2X_2]$, in high yields (Scheme 1).[2] An M/L ratio of 1:4 was found to be optimal for this reaction, as the excess ligand can act as the requisite base. The helicates readily crystallize from either MeOH or MeCN, greatly facilitating their isolation and purification, though hindering their characterization in solution. This latter point contrasts with hydrogen-bonded helicates prepared from ligand (*R*)-**2**, which, though also amenable to the synthetic procedures described above, show good solubility in polar solvents.

**Reaction of Ligands 1 and 2 with Copper(II) Salts.** The reaction of **1** with either $CuCl_2$ or $CuBr_2$ (4:1 ratio) in MeOH produces pale green crystalline solids that were identified by X-ray crystallography as the hydrogen-bonded helicates $[Cu_2(\mathbf{1})_2(\mathbf{1}-H)_2Cl_2]$ and $[Cu_2(\mathbf{1})_2(\mathbf{1}-H)_2Br_2]$. The structure of $[Cu_2(\mathbf{1})_2(\mathbf{1}-H)_2Br_2]$ is shown in Figure 1, and that of $[Cu_2(\mathbf{1})_2(\mathbf{1}-H)_2Cl_2]$ is shown in Figure S1.

Both the molecular structure and crystal packing arrangement of $[Cu_2(\mathbf{1})_2(\mathbf{1}-H)_2Cl_2]$ and $[Cu_2(\mathbf{1})_2(\mathbf{1}-H)_2Br_2]$ are nearly identical to their cobalt(II) counterparts (Table 1). In both instances, the geometry at the individual metal centers is approximately trigonal bipyramidal, as indicated by trigonality factors[18] ($\tau$) that approach unity, with the major axis defined by the N−Cu−N vector. The hydrogen bonds between the oxygen atoms of two molecules of **1** that build up the ligand strands exhibit similar O−H−O distances. It is notable that although the copper(II) and cobalt(II) complexes crystallize in different space groups, similar rows of helicates arranged in an 'end to end' fashion are observed along one of the crystallographic axes (*c* axis for Cu; *b* axis for Co). These rows are homochiral, i.e., they are composed of helicates of the same handedness.

We were interested to see whether we could prepare dinuclear copper(II) H-bonded helicates, $[Cu_2(\mathbf{1})_2(\mathbf{1}-H)_2X_2]$, that feature chiral ancillary ligands (X) coordinated to the metal ions. We reasoned that the lactate ion was a good

(6) Lane, T. J.; Kanadathil, A. J.; Rosalie, S. M. *Inorg. Chem.* **1964**, *3*, 487−490.
(7) Cheng, S.-C.; Wei, H.-H. *Inorg. Chim. Acta* **2002**, *340*, 105−113.
(8) Mueller, B.; Schneider, A.; Tesmer, M.; Vahrenkamp, H. *Inorg. Chem.* **1999**, *38*, 1900−1907.
(9) Canada-Vilalta, C.; Rumberger, E.; Brechin, E. K.; Wernsdorfer, W.; Folting, K.; Davidson, E. R.; Hendrickson, D. N.; Christou, G. *J. Chem. Soc., Dalton Trans.* **2002**, 4005−4010.
(10) Yoo, J.; Yamaguchi, A.; Nakano, M.; Krzystek, J.; Streib, W. E.; Brunel, L.-C.; Ishimoto, H.; Christou, G.; Hendrickson, D. N. *Inorg. Chem.* **2001**, *40*, 4604−4616.
(11) Yilmaz, V. T.; Guney, S.; Andac, O.; Harrison, W. T. A. *Polyhedron* **2002**, *21*, 2393−2402.
(12) Suzuki, Y.; Tomizawa, H.; Miki, E. *Inorg. Chim. Acta* **1999**, *290*, 36−43.
(13) Yilmaz, V. T.; Hamamci, S.; Thone, C. *Polyhedron* **2004**, *23*, 841−848.
(14) Harden, N. C.; Bolcar, M. A.; Wernsdorfer, W.; Abboud, K. A.; Streib, W. E.; Christou, G. *Inorg. Chem.* **2003**, *42*, 7067−7076.
(15) Yang, E.-C.; Hendrickson, D. N.; Wernsdorfer, W.; Nakano, M.; Zakharov, L. N.; Sommer, R. D.; Rheingold, A. L.; Ledezma-Gairaud, M.; Christou, G. *J. Appl. Phys.* **2002**, *91*, 7382−7384.
(16) Brechin, E. K.; Knapp, M. J.; Huffman, J. C.; Hendrickson, D. N.; Christou, G. *Inorg. Chim. Acta* **2000**, *297*, 389−399.
(17) Ito, M.; Onaka, S. *Inorg. Chim. Acta* **2004**, *357*, 1039−1046.
(18) Addison, A. W.; Rao, T. N.; Reedijk, J.; Rijn, J. V.; Verschoor, G. C. *J. Chem. Soc., Dalton Trans.* **1984**, 1349.

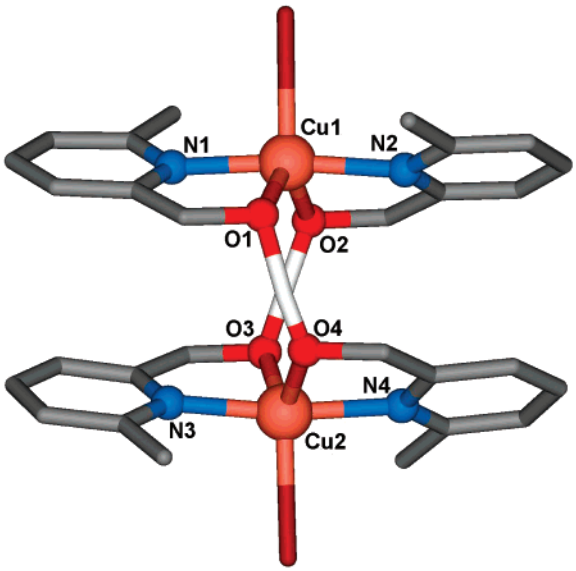


**Figure 1.** X-ray crystal structure of the $[Cu_2(\mathbf{1})_2(\mathbf{1}-H)_2Br_2]$ hydrogen-bonded helicate. Hydrogen atoms have been omitted for clarity. Selected distances (Å): Cu1−N1 = 2.040(16); Cu2−N1 = 1.994(15); Cu1−O1 = 2.036(12); Cu1−O2 = 1.974(12); Cu−Br = 2.5516(2); O1−H−O4 = 2.396; O2−H−O3 = 2.448; Cu1···Cu2 = 4.316. Selected angles (deg): N1−Cu1−O1 = 82.2(8); N1−Cu1−N2 = 173.7(5); O1−Cu1−O2 = 122.8-(4); Br1−Cu1−O1 = 122.4(4).

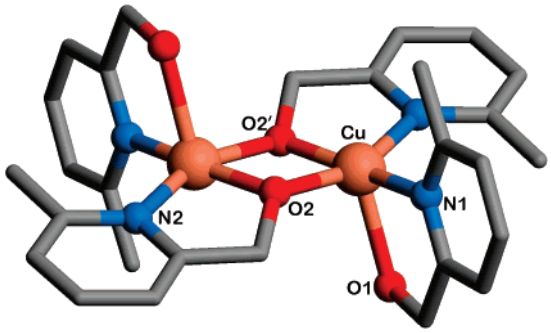


**Figure 2.** X-ray crystal structure of the centrosymmetric dimer $[Cu_2(\mathbf{1})_2(\mathbf{1}-H)_2](ClO_4)_2$. Hydrogen atoms and counterions are omitted for clarity. Selected distances (Å): Cu−N1 = 1.983(2); Cu−N2 = 2.029(2); Cu−O1 = 2.289(2); Cu−O2 = 1.9051(19); Cu−O2′ = 1.9541(19); Cu···Cu = 3.0200(7). Selected angles (deg): Cu−O2−Cu = 102.98(9); O2−Cu−O2′ = 77.02(9); N1−Cu−O2 = 167.34(9); N1−Cu−O1 = 76.46(9); N2−Cu−O2 = 82.61(9); N1−Cu−N2 = 107.35(9).

**Table 1.** Comparison of Selected Key Parameters in the X-ray Crystal Structures of $[Cu_2(\mathbf{1})_2(\mathbf{1}-H)_2Cl_2]$, $[Cu_2(\mathbf{1})_2(\mathbf{1}-H)_2Br_2]$, and $[Co_2(\mathbf{1})_2(\mathbf{1}-H)_2Br_2]$

| | $[Cu_2(\mathbf{1})_2(\mathbf{1}-H)_2Cl_2]$ | $[Cu_2(\mathbf{1})_2(\mathbf{1}-H)_2Br_2]$ | $[Co_2(\mathbf{1})_2(\mathbf{1}-H)_2Br_2]$ |
|---|---|---|---|
| cryst syst | monoclinic | monoclinic | orthorhombic |
| space group | $P2_1/c$ | $P2_1/c$ | *Pbcn* |
| | | Selected Distances (Å) | |
| M···M | 4.45 | 4.32 | 4.37 |
| O−H−O | 2.43, 2.46 | 2.40, 2.45 | 2.43 |
| M−N | 2.01−2.03 | 1.99 − 2.05 | 2.13, 2.15 |
| M−O | 2.01−2.07 | 1.97 − 2.04 | 1.99, 2.00 |
| M−X | 2.34 | 2.52, 2.55 | 2.47 |
| | | Selected Angles (deg) | |
| N−M−N | 171.7, 173.7 | 170.4, 173.7 | 167.2, 172.8 |
| O−M−O | 116.2, 117.5 | 115.8, 121.3 | 114.0, 118.7 |
| | | Trigonality factors ($\tau$)[18] | |
| | 0.73, 0.80 | 0.86, 0.81 | 0.74 |

candidate for the role of the ancillary ligand, as it is monoanionic, readily available in an enantiopure form, and is potentially able to bind to the copper(II) centers without disturbing helicate formation (analogous cobalt(II) helicates form with a variety of mono- and bidentate ancillary ligands[2]). To this end, $Cu(ClO_4)_2$, **1**, and lithium lactate (1:2:1 ratio) were combined in MeOH, resulting in the formation of green platelike crystals. Instead of the desired lactate-containing structure, however, X-ray crystallography revealed the dimeric complex $[Cu_2(\mathbf{1})_2(\mathbf{1}-H)_2](ClO_4)_2$ (Figure 2). This dimer is centered on a crystallographic inversion center in the space group $P2_1/c$ and comprises a pair of distorted square pyramidal copper(II) ions ($\tau = 0.18$) that are bridged by the O donors of two $\mu^2$-(**1**−H) ligands. A further bidentate ligand **1** completes the coordination sphere of each metal center, and the 2+ charge on the dimer is balanced by two non-coordinating $ClO_4^-$ counterions. The coordination geometry of the copper(II) ions is best described as slightly distorted square pyramidal, and the separation between the two copper nuclei is 3.0200(7) Å. Once the identity of this complex had been established, we were able to deliberately synthesize it via the reaction of **1**, $Cu(ClO_4)_2$, and $NEt_3$ in MeOH. It is noteworthy that a series of copper(II) dimers with a similar $[Cu_2L_2]$ platform has been reported in the literature.[7] These complexes are functional mimics of catecholase, an enzyme known to have a dimeric copper(II) motif at its active site.[19]

**Reaction of (*R*)-2 with $CuCl_2$ and $CuBr_2$.** Ligand (*R*)-**2** was combined with $CuCl_2$ in MeOH (4:1 ratio), and slow evaporation at room temperature led to the formation of a pale blue-green crystalline solid. As expected, X-ray crystallography revealed an enantiomorphous space group ($P2_1$). The molecular structure (Figure 3a, Table 2) features a mononuclear complex, $[Cu(\mathbf{2})_2Cl]Cl$, in which a copper(II) ion is coordinated to two bidentate (*R*)-**2** ligands and one chloro ligand with a distorted trigonal bipyramidal geometry. A chloride ion serves as the counteranion. The copper(II) center in $[Cu(\mathbf{2})_2Cl]^+$ represents a stereogenic center due to the skewed arrangement of the two chelating ligands. The absolute configuration at this center can thus potentially be either Δ or Λ;[20] however, the point chirality of the *R*-**2** ligand is observed to enforce the Λ absolute configuration in the solid state.

Of the two coordinated OH groups of ligand **2** in the $[Cu(\mathbf{2})_2Cl]^+$ cation, one is hydrogen bonded to the chloride counteranion (O−H···Cl = 3.01 Å) and the other is hydrogen bonded to the guest $H_2O$ molecule (O−H···O = 2.54 Å), as depicted in Figure 3b. A further pair of hydrogen bonds links the chloride ion to the guest $H_2O$ molecule (O−H···Cl = 3.07 and 3.12 Å), resulting in an infinite (H−O−H···Cl···H−O−H)$_\infty$ chain that spirals along the crystallographic *b* axis. This chain describes a left-handed helix.

The reaction of (*R*)-**2** with $CuBr_2$ in MeOH (either 2:1 or 4:1 ratio) leads to the lime green complex Λ,Λ-$[Cu_2(\mathbf{2})_3(\mathbf{2}\text{-}H)Br_2]Br$ (Figure 4, Table 2), which crystallizes in the space group $P2_1$. This dinuclear complex comprises two

(19) Gerdemann, C.; Eicken, C.; Krebs, B. *Acc. Chem. Res.* **2002**, *35*, 183−191.
(20) Von Zelewsky, A. *Stereochemistry of Coordination Compounds*; Wiley: Chichester, 1996.

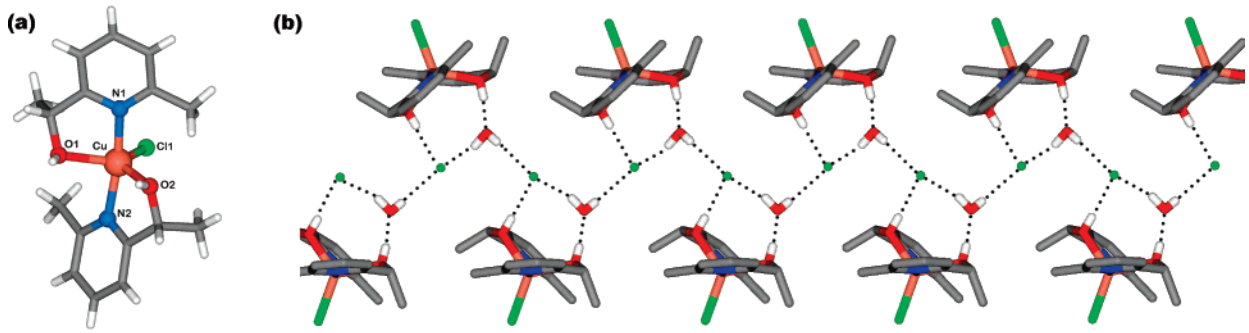


**Figure 3.** (a) X-ray crystal structure of the cation of Λ-[Cu(**2**)$_2$Cl]Cl. (b) The hydrogen-bonded (Cl···H−O−H···Cl···H−O−H)$_\infty$ chain that runs along the crystallographic *b* axis in [Cu(**2**)$_2$Cl]Cl. Selected distances (Å): Cu−N1 = 2.006(2); Cu−N2 = 2.012(2); Cu−O1 = 2.106(2); Cu−O2 = 2.092(2); Cu−Cl = 2.2534(7). Selected angles (deg): N1−Cu−O1 = 80.55(8); N2−Cu−O2 = 80.88(9); N1−Cu−N2 = 164.88(8); O1−Cu−O2 = 112.82(8); O1−Cu−Cl1 = 125.87(6); O2−Cu−Cl2 = 121.30(6).

**Table 2.** Comparison of the X-ray Crystal Structures of [Cu(**2**)$_2$Cl]Cl and [Cu$_2$(**2**)$_2$(**2**-H)$_2$Br$_2$]Br

| | [Cu(**2**)$_2$Cl]Cl | [Cu$_2$(**2**)$_3$(**2**−H)Br$_2$]Br |
|---|---|---|
| cryst syst | monoclinic | monoclinic |
| space group | $P2_1$ | $P2_1$ |
| | Selected Distances (Å) | |
| Cu−N | 2.00, 2.01 | 1.99 − 2.03 |
| Cu−O | 2.09, 2.11 | 1.96, 2.19[a] |
| Cu−X | 2.25 | 2.42, 2.45 |
| Cu···Cu | − | 5.61 |
| O−H−O | − | 2.40, 2.45 |
| | Selected Angles (deg) | |
| N−Cu−N | 164.9 | 167.7, 169.8 |
| O−Cu−O | 112.8 | 104.3, 111.6 |
| | Trigonality Factors ($\tau$) | |
| | 0.65 | 0.61, 0.38 |

[a] The Cu−O bond to the O atom involved in the interligand H-bond is markedly shorter than the other Cu−O bond.

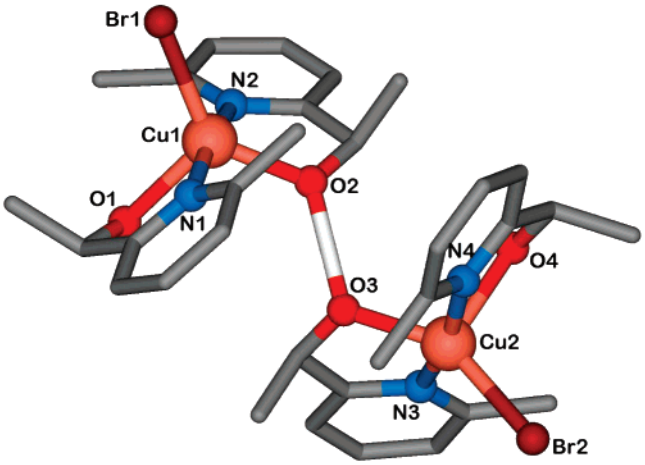


**Figure 4.** Structure of the [Cu$_2$(**2**)$_3$(**2**-H)Br]$^+$ cation as determined by X-ray crystallography. Hydrogen atoms omitted for clarity. Selected distances (Å): Cu1−N1 = 2.027(2); Cu1−N2 = 2.021(2); Cu1−O1 = 2.191(2); Cu1−O2 = 1.9635(18); Cu1−Br1 = 2.4208(4); O2−O3 = 2.413; Cu1···Cu2 = 5.610. Selected angles (deg): N1−Cu1−O1 = 77.19(10); N1−Cu1−N2 = 167.74(9); O1−Cu1−O2 = 104.30(9); O1−Cu1−Br1 = 109.94(7).

five-coordinate {Cu(**2**)$_2$Br} units that are linked by a single hydrogen bond (O−H−O separation = 2.41 Å). The geometries of the individual {Cu(**2**)$_2$Br} units are subtly different (Table 2); however, both adopt the Λ absolute configuration.

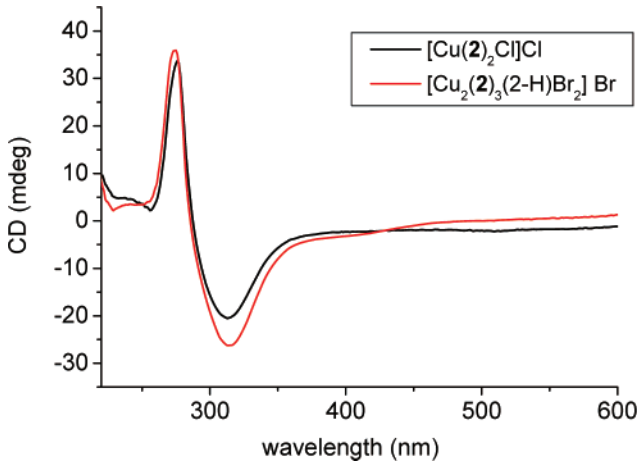


**Figure 5.** Solid-state CD spectra of [Cu(**2**)$_2$Cl]Cl (black line) and [Cu$_2$(**2**)$_3$(**2**-H)Br$_2$]Br (red line), recorded as KBr discs.

The above-mentioned hydrogen bond that links the {Cu(**2**)$_2$Br} monomers effectively produces a bis(bidentate) ligand strand. This ligand strand does not, however, twist around the Cu···Cu axis; therefore, the [Cu$_2$(**2**)$_3$(**2**-H)Br$_2$]$^+$ assembly cannot properly be described as a helicate. It is unclear why a second hydrogen bond does not form between O1 and O4 (Figure 4) to produce a hydrogen-bonded helicate akin to that previously observed following the reaction of (*R*)-**2** with CoBr$_2$ and the reaction of **1** with CuBr$_2$.

The CD spectra of Λ-[Cu(**2**)$_2$Cl]Cl and Λ,Λ-[Cu$_2$(**2**)$_3$(**2**-H)Br$_2$]Br, recorded in the solid state as KBr discs, are presented in Figure 5. The two spectra are nearly identical: a negative peak around 313 nm and a positive peak around 275 nm are observed in both cases. These two spectra share a close resemblance to those of [Co$_2$(**2**)$_2$(**2**-H)$_2$X$_2$] (X = Cl$^-$, Br$^-$). The major differencs are that the spectra of the copper(II) complexes lack prominent bands in the visible region and their negative peak at around 313 nm is of comparable magnitude to the positive peak at 275 nm; the negative peak is much less intense for the cobalt(II) helicates.

The above observations suggest that the observed CD activity of [Cu(**2**)$_2$Cl]Cl and [Cu$_2$(**2**)$_3$(**2**-H)Br$_2$]Br arises from transitions localized on the pyridyl-alcohol ligands (rather than charge-transfer transitions). Furthermore, this signal can presumably be ascribed to local effects at the individual mononuclear units rather than to any long-distance effects

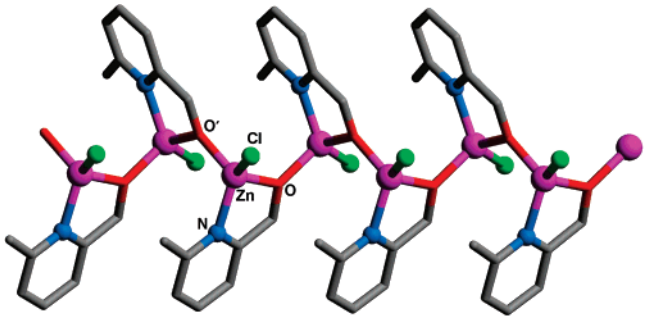


**Figure 6.** X-ray crystal structure of the helical $[Zn(\mathbf{1}-H)Cl]_\infty$ coordination polymer. Selected distances (Å): Zn−N = 2.047(2); Zn−O = 1.961(2); Zn−O′ = 1.934(2); Zn−Cl = 2.2115(8). Selected angles (deg): N−Zn−O = 83.32(9); N−Zn−O′ = 110.63(10); N−Zn−Cl = 125.95(7); Zn−O−Zn = 125.18(10).

such as exciton coupling between chromophores coordinated to different metal centers (internuclear exciton coupling)[21] or chromophores on neighboring complexes (intermolecular exciton coupling). Although the distance between chromophores located on different metal centers and neighboring complexes is relatively short and could in theory allow for such effects to be operative, they may be precluded by the relative weakness of the electronic transitions associated with these complexes (the strength of exciton coupling is proportional to the square of the absorptivity coefficient).[22] The inherent difficulty of computing the excited state properties of open-shell $d^9$ systems discouraged us from developing a theoretical model of this system.

**Reaction of 1 with $ZnCl_2$ and $ZnBr_2$.** The reaction of ligand **1** with $ZnCl_2$ (4:1 ratio) in MeOH led to the formation of colorless crystals, and analysis by X-ray crystallography gave the structure shown in Figure 6. The crystal was found to comprise a 1-D polymer of [Zn(**1**−H)Cl] units. Each zinc ion is coordinated to a chelating **1**-H ligand, a chloride ligand, and the O donor of a neighboring [Zn(**1**−H)Cl] unit in a highly distorted tetrahedral geometry. This bridging O donor mediates the formation of infinite helical chains that extend along the crystallographic *a* axis. Although the structure was solved in the non-centrosymmetric space group $P2_12_12_1$, it was more satisfactorily refined as a racemic twin, i.e., the crystal comprises domains of left- and right-handed helices.

$[Zn(\mathbf{1}-H)Cl]_\infty$ could also be synthesized via the reaction of **1**, $ZnCl_2$, and $NEt_3$ (1:1:1 ratio) in MeOH and via the reaction of **1**, $ZnCl_2$, and $Zn(OAc)_2$ (2:1:1 ratio) in MeOH. Furthermore, the use of $ZnBr_2$ in place of $ZnCl_2$ led to an analogous coordination polymer, as evidenced by elemental analysis and IR spectroscopy. Neither solid was observed to fluoresce under excitation with UV light.

**Reaction of 1 with Nickel(II) Salts.** The reaction of $NiCl_2{\cdot}6H_2O$ with ligand **1** (1:4 ratio) in MeOH led to the formation of a pale green crystalline solid, and analysis of a selected single crystal by X-ray crystallography gave the $[Ni_4(\mathbf{1}-H)_4Cl_4(MeOH)_4]$ cubane structure shown in Figure 7. Elemental analysis of a bulk sample of this compound

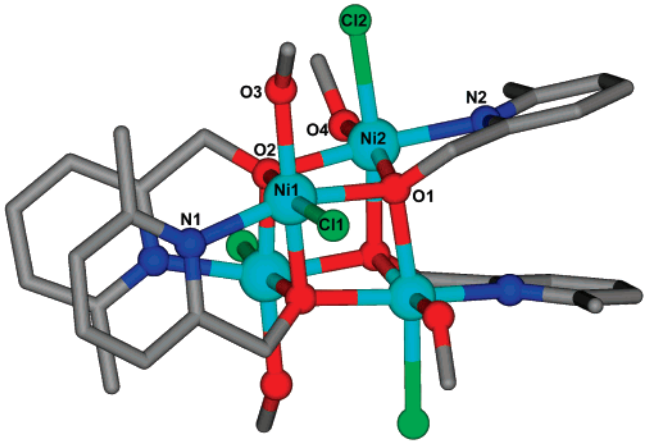


**Figure 7.** X-ray crystal structure of $[Ni_4(\mathbf{1}-H)_4Cl_4(MeOH)_4]$. A crystallographic $C_2$ axis runs through the center of the cubane. Selected distances (Å): Ni1−N1 = 2.115(4); Ni1−O1 = 2.065(2); Ni−O3 = 2.070(3); Ni1−Cl1 = 2.409(1); Ni1···Ni2 = 3.114; Ni1···Ni1′ = 3.151. Selected angles (deg): N1−Ni1−O2 = 80.12(11); Ni1−O1−Ni2 = 99.31(10); O1−Ni1−O2 = 80.66(9).

did not correspond to $[Ni_4(\mathbf{1}-H)_4Cl_4(MeOH)_4]$ (or any reasonable solvates) but did closely match $[Ni_4(\mathbf{1}-H)_4Cl_4(H_2O)_4]$. This presumably indicates that drying of the compound in an oven at 40 °C prior to elemental analysis leads to the replacement of the MeOH ligands by $H_2O$. The yield of the cubane could be improved by using a metal/ligand ratio of 1:1.

$[Ni_4(\mathbf{1}-H)_4Cl_4(MeOH)_4]$ crystallizes in the space group *C*2/*c* with a crystallographic 2-fold axis running through its center. The four nickel(II) ions are located at the diagonally opposed corners of a cubane, with triply bridging O donor atoms of the **1**−H ligand filling the remaining four vertices. A chloride anion and a MeOH molecule complete the coordination spheres of the nickel(II) ions, which have a near-octahedral coordination geometry. The overall structure of this complex is reminiscent of the previously investigated $[Co_4(\mathbf{1}-H)_4Cl_4(H_2O)_3(MeOH)]$ cubane.[3]

Isele et al. have analyzed the crystal structures of a large number of cubanes found in the Cambridge Structural Database and have developed a system to describe the distortions in the core $M_4O_4$ unit based on the M···M and O···O distances.[23] The Ni···Ni distances in $[Ni_4(\mathbf{1}-H)_4Cl_4(MeOH)_4]$ range from 3.114 to 3.156 Å, with a mean of 3.141 Å and a standard deviation of 0.021 Å, while the O···O distances range from 2.635 to 2.695 Å, with a mean of 2.664 Å and a standard deviation of 0.018 Å. Analysis of these data using the Isele method shows that $[Ni_4(\mathbf{1}-H)_4Cl_4(MeOH)_4]$ has a slight $S_4$ distortion, i.e., the tetrahedron described by the four metal ions is slightly distorted by extension along one of its $S_4$ axes.

A related experiment was performed where ligand **1** was reacted with $NiCl_2{\cdot}6H_2O$ and $Ni(OAc)_2{\cdot}4H_2O$ (1:1:4 ratio) in MeOH. The analogous reaction involving cobalt(II) salts has been shown to lead to H-bonded helicates, with the acetate ions acting as a base.[2] In the case of nickel(II), however, a tetranuclear cubane, $[Ni_4(\mathbf{1}-H)_4Cl_2(OAc)_2$-

(21) Telfer, S. G.; Tajima, N.; Kuroda, R. *J. Am. Chem. Soc.* **2004**, *126*, 1408−1418.
(22) Rodger, A.; Norden, B. *Circular Dichroism and Linear Dichroism*; Oxford University Press: Oxford, 1997.
(23) Isele, K.; Gigon, F.; Williams, A. F.; Bernardinelli, G.; Franz, P.; Decurtins, S. *Dalton Trans.* **2007**, 332−341.

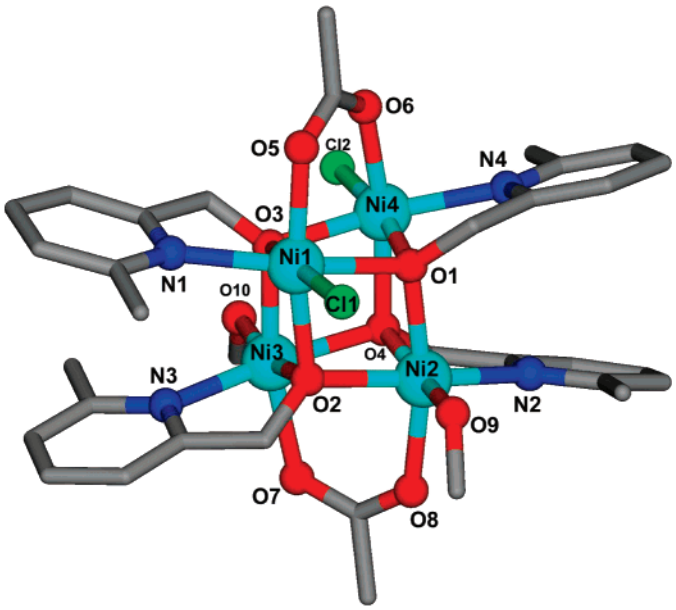


**Figure 8.** X-ray structure of one of the two isomeric $[Ni_4(\mathbf{1}-H)_4Cl_2(OAc)_2(MeOH)_2]$ tetranuclear cubanes (isomer A) found in the same crystal. Isomer B can be envisaged by switching Cl1 and the O9-containing MeOH ligand (see text and Figure S2). Selected distances (Å): Ni1−N1 = 2.162(6); Ni1−O1 = 2.069(4); Ni−O3 = 2.036(5); Ni1−Cl1 = 2.374(2); Ni1−O5 = 2.044(5); Ni1···Ni3 = 3.119; Ni1···Ni4 = 2.979. Selected angles (deg): N1−Ni1−O3 = 78.13(20); O1−Ni1−O2 = 78.42(19); Ni1−O1−Ni2 = 101.88(19); Ni1−O3−Ni3 = 99.47(19).

$(MeOH)_2]$, was observed to form. $[Ni_4(\mathbf{1}-H)_4Cl_2(OAc)_2(MeOH)_2]$ crystallizes in the space group $Pca2_1$ with the asymmetric unit comprising two distinct tetranuclear clusters. These clusters are diastereoisomers, which differ in the relative arrangements of their two chloro and two MeOH ligands. For the isomer that is presented in Figure 8 (isomer A), the two chloro ligands of the cubane are bound to two nickel(II) ions that are bridged by one of the acetate ligands, and the two MeOH ligands coordinate to the two nickel(II) ions that are bridged by the second acetate ligand. In this isomer a pseudo-$C_2$ axis is roughly defined by the two C−$CH_3$ bonds of the two acetate ligands. The structure of the second isomer (isomer B) can be conceptualized by switching the Cl1 ligand and the O9-containing MeOH ligand (Figure S2). The acetate ligands in this isomer form bridges between a nickel(II) ion that coordinates to a chloro ligand and a nickel(II) ion that coordinates to a MeOH ligand, and it has a pseudo-$C_2$ axis that passes through the two faces of the cubane that support the **1** ligands.

The Ni···Ni distances in isomer A of $[Ni_4(\mathbf{1}-H)_4Cl_2(OAc)_2(MeOH)_2]$ range from 2.925 to 3.200 Å (standard deviation = 0.116 Å), and the spread of distances in isomer B is quite similar (2.924−3.203 Å, standard deviation = 0.127 Å). For both isomers, the shortest Ni···Ni distances correspond to the metal centers that are bridged by the acetate ligands, and this leads to a distinct puckering of the cubanes, which destroys most of the ideal $T_d$ symmetry of the $Ni_4O_4$ core.

**Reaction of 1 with $MnCl_2$.** $MnCl_2{\cdot}4H_2O$ and **1** (1:4 ratio) were combined in MeOH, and dark-red crystals were observed to form over a period of several weeks at room temperature. These crystals were subjected to X-ray crystallography, which demonstrated that the known mixed-valence $Mn^{II}/Mn^{III}$ cluster complex, $[Mn_4(\mathbf{1}-H)_6Cl_4]$, had formed.[10]

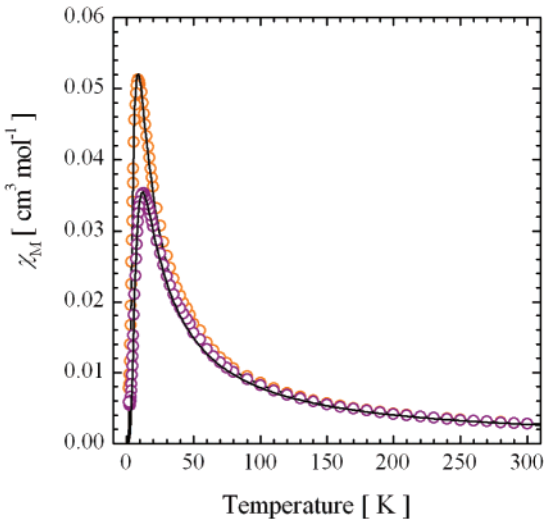


**Figure 9.** Magnetic susceptibility, $\chi_M$, of $[Cu_2(\mathbf{1})_2(\mathbf{1}-H)_2X_2]$ as a function of temperature (X = Cl, orange; X = Br, purple). Solid lines correspond to the fit to the Bleaney−Bowers equation.

**Magnetic Properties.** The magnetic susceptibility, $\chi_M$, of $[Cu_2(\mathbf{2})_3(\mathbf{2}\text{-H})Br_2]Br$ was determined upon cooling from 300 to 1.8 K. It increases steadily until 1.8 K, following the Curie Law between 300 and 10 K. The $\chi_M T$ product has a value of 0.79 cm$^3$ K mol$^{-1}$ at 300 K and remains constant until 10 K (Figure S11). Below this temperature, a slight decrease is observed. The value of $\chi_M T$ at room temperature is consistent with two isolated $S = 1/2$ centers (0.75 cm$^3$ K mol$^{-1}$).

The lack of any maximum in $\chi_M$ and the negligible drop in $\chi_M T$ indicate that almost no magnetic coupling exists between the metal centers in $[Cu_2(\mathbf{2})_3(\mathbf{2}\text{-H})Br_2]Br$. This can be attributed to a poor overlap of the $d_{z^2}$ magnetic orbitals and the presence of a single hydrogen-bond bridge, which reduces possible coupling pathways. The overall geometry also places the copper(II) centers a long 5.61 Å apart.

The temperature dependence of $\chi_M$ was also determined for $[Cu_2(\mathbf{1})_2(\mathbf{1}-H)_2X_2]$ (X = Cl, Br), as shown in Figure 9. A maximum can be observed at 8.5 and 12.5 K for the chlorine and bromine analogues, respectively. The $\chi_M T$ product for both complexes was found to be constant between 300 and 50 K at a value of 0.84 cm$^3$ K mol$^{-1}$. Below 50 K, a steep drop in $\chi_M T$ is observed and values of 0.014 and 0.010 cm$^3$ K mol$^{-1}$ are reached at 1.8 K for the chlorine- and bromine-containing dimers, respectively. Although the room-temperature $\chi_M T$ product is consistent with two isolated paramagnetic $S = 1/2$ centers, the large drop in $\chi_M T$ and the maximum in $\chi_M$ suggest that significant antiferromagnetic coupling between the copper(II) centers in both dimers exists. The susceptibility of both complexes was fit to the Bleaney−Bowers[24] equation:

$$\chi_M = \frac{2N_A g^2 \mu_B{}^2}{k_B T[3 + \exp(-J/k_B T)]}$$

where $J$ is the coupling constant between the two copper(II)

(24) Bleaney, B.; Bowers, K. D. *Proc. R. Soc. London A* **1952**, *214*, 451.

centers. This fit yielded $J = -4.60(4)$ cm$^{-1}$ ($g = 2.14(2)$) for $[Cu_2(\mathbf{1})_2(\mathbf{1}-H)_2Cl_2]$and $J = -6.51(7)$ cm$^{-1}$ ($g = 2.10(2)$) for $[Cu_2(\mathbf{1})_2(\mathbf{1}-H)_2Br_2]$.

Magnetic interactions between the copper(II) centers in both $[Cu_2(\mathbf{1})_2(\mathbf{1}-H)_2X_2]$ dimers are likely to be mediated through the hydrogen bonds along the two Cu−O−H···O−Cu bridges. The double bridge in $[Cu_2(\mathbf{1})_2(\mathbf{1}-H)_2X_2]$ probably helps to support shorter Cu···Cu (4.32 (Cl) and 4.45 (Br) Å) distances compared to the singly bridged $[Cu_2(\mathbf{2})_3(\mathbf{2}\text{-H})Br_2]Br$. The bridging motif in $[Cu_2(\mathbf{1})_2(\mathbf{1}-H)_2X_2]$ also aligns the equatorial planes to afford better overlap of the magnetic molecular orbitals, thereby increasing the coupling strength. The slightly stronger coupling in the bromo complex could be due to its shorter M−O and O−H···O distances as compared with the chloro analogue (Table 1). However, the multi-atom length of this bridge is presumably responsible for the relatively weak coupling constants in these dimers compared to one-atom (such as alkoxo, hydroxo, oxo or halo) bridged copper(II) dimers.[25−27]

Considering the structure of $[Cu_2(\mathbf{1})_2(\mathbf{1}-H)_2X_2]$, these magnetic data represent a clear determination of the potential strength of hydrogen bond-mediated coupling between metal centers. A similar coupling constant (−3.18(9) cm$^{-1}$) was reported for the analogous $[Co_2(\mathbf{1})_2(\mathbf{1}-H)_2Cl_2]$ hydrogen-bonded helicate,[3] which exhibited a maximum in susceptibility in the vicinity of 6 K. The $J$ values found for $[Cu_2(\mathbf{1})_2(\mathbf{1}-H)_2X_2]$ are, however, free of any orbital contribution to the magnetic moment. Several other examples of copper(II) dimers bridged via a hydrogen bond have been reported, most showing antiferromagnetic interactions.[28,29] Theoretical studies have shown that interactions could be mediated in these square pyramidal, Jahn−Teller distorted square bipyramidal or square planar copper(II) dimers through hydrogen bonds.[29] Hydrogen bond-mediated magnetic interactions have been probed for organic radical-based materials and have been found to be responsible for low-temperature magnetic ordering in some cases.[30,31]

The magnetic susceptibility of $[Cu_2(\mathbf{1})_2(\mathbf{1}-H)_2](ClO_4)_2$ was measured between 350 and 1.8 K. Upon cooling, $\chi_M$ was found to decrease slowly and below 90 K it became negative, i.e., the system was effectively diamagnetic (Figure S12). At 300 K, a $\chi_M T$ value of 0.42 cm$^3$ K mol$^{-1}$ was determined per copper(II) dimer. This small value (versus the expected 0.75 cm$^3$ K mol$^{-1}$), along with the broad maximum in $\chi_M$ around 325−350 K, indicates that strong antiferromagnetic coupling occurs at room temperature. The $\chi_M$ vs $T$ curve

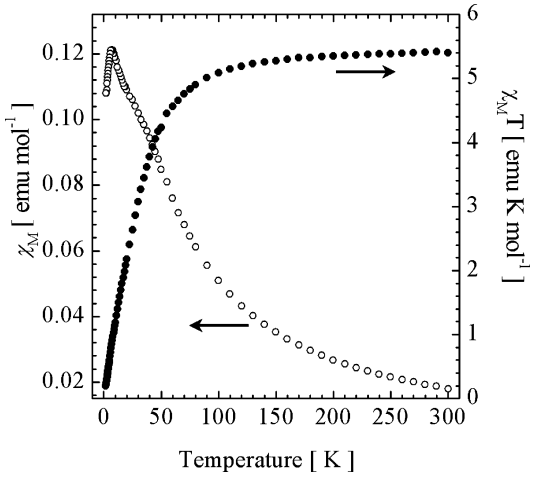


**Figure 10.** Magnetic susceptibility, $\chi_M$, (empty circles) and $\chi_M T$ product (filled circles) for $[Ni_4(\mathbf{1}-H)_4Cl_2(OAc)_2(MeOH)_2]$ as a function of temperature.

was fit to the Bleaney−Bowers equation[24] to yield $J = -377(5)$ cm$^{-1}$ and $g = 1.97(2)$.

The presence in $[Cu_2(\mathbf{1})_2(\mathbf{1}-H)_2](ClO_4)_2$ of a short one-atom bridge (Cu−O = 1.90−1.95 Å) between the copper(II) ions, as well as an essentially coplanar equatorially bridged core is responsible for the large coupling. Similar alkoxo-bridged copper(II) dimers were also reported to be antiferromagnetically coupled, with large coupling constants.[7] However, no clear trend can be drawn between the Cu···Cu distances, the Cu−O−Cu angles and the coupling constants observed for these alkoxo-bridged dimers. The backbone of the alkoxo-amine ligand, as well as the other ligands bound on the copper(II) centers, affect the overall geometry of these dimers and, as a consequence, the magnetic pathways are different. More data on a series of structurally related systems would be required in order to construct magneto-structural correlations.

The magnetic susceptibility and the $\chi_M T$ product were determined for $[Ni_4(\mathbf{1}-H)_4Cl_2(OAc)_2(MeOH)_2]$ as a function of temperature (Figure 10). At 300 K, the $\chi_M T$ value is equal to 5.40 cm$^3$ K mol$^{-1}$, and it remains nearly constant down to 150 K. Below 150 K, the $\chi_M T$ product decreases steadily, and a value of 0.19 cm$^3$ K mol$^{-1}$ is reached at 1.8 K. A maximum is present in the $\chi_M$ vs $T$ plot at 7.5 K, as well as a shoulder around 25 K. These data are consistent with significant antiferromagnetic interactions between the nickel(II) centers in the $Ni_4O_4$ cubane core. However, the data were not modeled further due to the presence of two stereoisomers of the $[Ni_4(\mathbf{1}-H)_4Cl_2(OAc)_2(MeOH)_2]$ cubane in the unit cell: slightly different superexchange pathways are present in each isomer, which preclude attempts to make accurate magneto-structural correlations. For example, the shoulder observed in $\chi_M$ could arise from stronger coupling in one $Ni_4O_4$ isomer versus the other. Nevertheless, it is clear that both isomers exhibit antiferromagnetic coupling and this can be compared with a few related $Ni_4O_4$ cubanes such as $[Ni_4((S,S)\text{-L}-H)_4](ClO_4)_4(H_2O)_5$, which show antiferromagnetic properties in the same temperature range.[23] In most of the other $Ni_4O_4$ cubanes, ferromagnetic coupling is observed. The type of magnetic interactions present in $M_4O_4$ cubane

(25) Chandramouli, G. V. R.; Kundu, T. K.; Manoharan, P. T. *Aust. J. Chem.* **2003**, *56*, 1239−1248.
(26) Hatfield, W. E. In *Magneto-Structural Correlations in Exchange Coupled Systems*; Willet, R. D., Gatteschi, D., Kahn, O., Eds.; Reidel: Dordrecht, The Netherlands, 1984; p 555.
(27) Katz, M. J.; Shorrock, C. J.; Batchelor, R. J.; Leznoff, D. B. *Inorg. Chem.* **2006**, *45*, 1757−1765.
(28) Plass, W.; Pohlmann, A.; Rautengarten, J. *Angew. Chem., Int. Ed.* **2001**, *40*, 4207−4210.
(29) Desplanches, C.; Ruiz, E.; Rodriguez-Fortea, A.; Alvarez, S. *J. Am. Chem. Soc.* **2002**, *124*, 5197−5205.
(30) Ren, X.; Chen, Y.; He, C.; Gao, S. J. *Dalton Trans.* **2002**, 3915−3918.
(31) Wernsdorfer, W.; Allaga-Alcade, N.; Hendrickson, D. N.; Christou, G. *Nature* **2002**, *416*, 406−409.

complexes was found to be related to the type of distortion present in the structure.[23]

## Conclusion

The primary aim of this study was to determine which late first row transition metal ions could form hydrogen-bonded helicates upon reaction with ligands **1** and **2**. The results show that, of the various metal salts investigated, only $CuCl_2$ and $CuBr_2$ produce helicates with ligand **1**, with the reaction of this ligand with $MnCl_2$, $NiCl_2$ and $ZnCl_2$ leading to either cubanes or coordination polymers. Given this success with $CuCl_2$ and $CuBr_2$, we attempted to synthesize related helicates with ligand **2**; however, this led to the formation of a mononuclear complex and a dinuclear dimer with a single hydrogen bond, respectively.

The formation of hydrogen-bonded helicates from **1** and **2** is clearly sensitive to the identity of the metal ion. It is difficult to rationalize why cobalt(II) and copper(II) produce helicates while the other metal ions do not. It is expected that the approximate trigonal bipyramidal geometry required for formation of the hydrogen-bonded helicates would be attainable by all the metal ions under investigation without significant energetic penalty. Ligand field stabilization effects may, however, favor nickel(II) complexes with octahedral geometries, and it is noteworthy that triple stranded hydrogen-bonded helicates that feature octahedral nickel(II) centers have previously been reported.[32] Such effects, however, would be of no consequence for manganese(II) and zinc(II). The size of the metal ions may be of some importance. For example, the Co−O and Cu−O bond lengths, which are observed to be approximately equal in the solid state, may optimize the acidity of the alcohol group of ligand **1** to promote the partial deprotonation required for hydrogen bond formation (as opposed to the full deprotonation required for cubane formation), although this remains rather speculative at this stage.

This investigation has focused on the solid-state structures and thus has an intrinsic bias toward less-soluble complexes; a quantitative solution-based study would be required attaining a full thermodynamic picture of the various accessible species.

For the moment, although our understanding of this system remains rather empirical, some useful ground rules have been developed on the basis of the above observations and in conjunction with earlier work.[2,3] It is apparent that hydrogen-bonded helicates only self-assemble from simple pyridine-alcohol ligands under a very narrow and specific set of conditions. Under these conditions, the use of noncovalent interactions to build up the ligands strands represents an extremely efficient method for the construction of these assemblies. Outside of these conditions, a varied array of alternative products are observed to form, highlighting the versatility of simple pyridine-alcohol ligands in metallosupramolecular chemistry.

(32) Kiriyama, H.; Fukuda, T.; Yamagata, Y.; Sekido, E. *Acta Crystallogr. C* **1985**, *41*, 1441.

## Experimental Section

**General.** Unless otherwise stated, chemicals were purchased from Wako, TCI, or Aldrich and were used as received. Ligand (*R*)-**2** was synthesized as described previously.[1] Microanalyses were performed by Toray Research Center, Tokyo, Japan, or the Campbell Microanalytical Laboratory, University of Otago, New Zealand. Solid-state CD spectra were measured as KBr discs on the purpose-built JASCO J800-KCM spectrophotometer[33] and were corrected for potential artefacts arising from linear dichroism (LD) and linear birefringence (LB) and the interaction between LD and LB of the sample and the nonideal characteristics of polarization modulation instrument.

**Magnetic Measurements**. Magnetic susceptibility data were collected for all samples using a Quantum Design MPMS-XL7 SQUID magnetometer equipped with an Evercool dewar working from 300 to 1.8 K under an applied magnetic field of 1 T. Polycrystalline samples were packed into gelatin capsules, which were then mounted in low-background diamagnetic plastic straws. The data were corrected for the diamagnetism of the constituent atoms using Pascal constants.[34]

**Synthetic Procedures. [$Cu_2$(1)$_2$(1−H)$_2Cl_2$].** $CuCl_2$ (65.5 mg, 0.49 mmol) was dissolved in MeOH (3 mL) and combined with a solution of **1** (240 mg, 1.95 mmol) in MeOH (2 mL). Pale blue-green prismatic crystals grew upon cooling the green solution to 4 °C overnight, and these were filtered off, washed with cold MeOH, and air-dried. Yield: 106 mg (60%). Anal. Calcd (Found) for [$Cu_2$(**1**)$_2$(**1**-H)$_2Cl_2$]·$CH_3OH$ ($C_{29}H_{38}Cl_2Cu_2N_4O_5$): C, 48.33 (48.5); N, 7.77 (7.8); H, 5.36 (5.4). IR (nujol): 3404 (m), 1609 (s), 1578 (m), 1279 (w), 1227 (w), 1173 (m), 1040 (br, m), 1032 (m), 1022 (s), 980 (br m), 787 (m) $cm^{-1}$.

**[$Cu_2$(1)$_2$(1−H)$_2Br_2$].** **1** (227 mg, 1.84 mmol) was dissolved in MeOH (1.5 mL) and $CuBr_2$ (103 mg, 0.46 mmol) was added to give an emerald green solution. Pale green prismatic crystals formed upon overnight refrigeration, and these were filtered off, washed with MeOH and $Et_2O$, and air-dried. Slow evaporation of the filtrate at room temperature produced a second crop of crystals. Total yield: 139 mg (78%). Anal. Calcd (Found) for [$Cu_2$(**1**)$_2$(**1**−H)$_2Br_2$] ($C_{28}H_{34}Br_2Cu_2N_4O_4$): C, 43.25 (42.7); H, 4.41 (4.5); N, 7.21 (6.8). IR (nujol): 3420 (m), 1609 (s), 1578 (m), 1260 (w), 1173 (m), 1030 (m), 1022 (s), 964 (br m), 787 (m) $cm^{-1}$.

**[$Cu_2$(1)$_2$(1−H)$_2$](ClO$_4$)$_2$·$H_2O$.** **1** (40.3 mg, 0.327 mmol) was dissolved in MeOH (0.5 mL) and combined with a mixture of Cu(ClO$_4$)$_2$·$6H_2O$ (60.6 mg, 0.162 mmol) and $NEt_3$ (22.5 $\mu$L, 0.162 mmol) in MeOH (0.5 mL). A green precipitate formed rapidly, which was filtered off and recrystallized from a mixture of hot MeOH (3 mL) and DMSO (0.8 mL). Emerald green crystals formed upon cooling to 20 °C, and these were filtered off, washed with cold MeOH, and air-dried. Yield: 34.9 mg (53%). Anal. Calcd (Found) for [$Cu_2$(**1**)$_2$(**1**-H)$_2$](ClO$_4$)$_2$ ($C_{28}H_{34}Cl_2Cu_2N_4O_{12}$): C, 41.29 (41.1); H, 3.96 (4.3); N, 6.88 (6.8). IR (nujol): 3310 (br, m), 1119 (s), 1043 (br s), 927 (m) $cm^{-1}$.

**Λ-[Cu(2)$_2$Cl]Cl.** A solution of (*R*)-**2** (17.5 mg, 0.13 mmol) in MeOH (0.5 mL) was combined with $CuCl_2$ (4.3 mg, 32 $\mu$mol) to give a pale green solution to which toluene (1 mL) was added. Slow evaporation over several days at room temperature produced large pale blue-green platelike needles. Yield: 9.7 mg (71%). Anal. Calcd (Found) for [Cu(**2**)$_2$Cl]Cl·$H_2O$ ($C_{16}H_{24}Cl_2CuN_2O_3$): C, 45.02 (45.2); H, 5.67 (5.7); N, 6.56 (6.4). IR (KBr disc): 3365 (s, br), 3000 (s, br), 2782 (m), 2680 (m), 2482 (w), 2362 (w), 2022 (w),

(33) Kuroda, R.; Harada, T.; Shindo, Y. *Rev. Sci. Instrum.* **2001**, *72*, 3802−3810.

(34) Kahn, O. *Molecular Magnetism*; VCH: Weinheim, 1993.

1928 (w), 1610 (s), 1576 (m), 1472 (s), 1450 (m), 1420 (w), 1373 (m), 1330 (m), 1292 (m), 1273 (m), 1237 (w), 1222 (m), 1167 (m), 1089 (s), 1073 (m), 1048 (m), 1028 (m), 1008 (m), 931 (m), 873 (w), 807 (m), 756 (w), 726 (w), 669 (w), 645 (w) $cm^{-1}$.

**Λ,Λ-[$Cu_2$(2)$_3$(2-H)$Br_2$]Br.** $CuBr_2$ (44.7 mg, 0.20 mmol) was dissolved in MeOH (1 mL) and added to a solution of (*R*)-**2** (54.9 mg, 0.40 mmol) in $CH_2Cl_2$ (1 mL). Toluene (2 mL) was added, and the green solution was evaporated slowly at room temperature to give lime green blocklike crystals, which were filtered off and washed with toluene and hexane. Yield: 35.7 mg (34%). Anal. Calcd (Found) for [$Cu_2$(**2**)$_3$(**2**-H)$Br_2$]Br·($H_2O$)·($CH_3OH$)·($CH_2Cl_2$) ($C_{34}H_{51}Br_3Cl_2Cu_2N_4O_6$): C, 38.91 (39.0); H, 4.90 (4.7); N, 5.34 (5.6). IR (KBr disc): 3354 (br, s), 3059 (br, s), 2976 (s), 2927 (s), 2676 (m), 2346 (m), 1609 (s), 1576 (s), 1470 (s), 1449 (s), 1374 (m), 1331 (m), 1286 (m) 1271(m), 1223 (m), 1168 (m), 1088 (s), 1047 (s), 1027 (s), 1005 (m), 931 (m) 872 (w), 804 (s), 755 (w), 725 (w), 644 (w) $cm^{-1}$.

**[Zn(1−H)Cl]$_\infty$. 1** (50 mg, 0.41 mmol) was dissolved in MeOH (2 mL) and combined with a solution of $ZnCl_2$ (13.8 mg, 0.10 mmol) in MeOH (1 mL). The colorless solution was left to sit at room temperature overnight to give a colorless crystalline solid that was filtered off, washed with MeOH and $Et_2O$, and air-dried. Yield: 7.1 mg (32%). Anal. Calcd (Found) for $C_7H_8ClNOZn$: C, 37.70 (37.8); H, 3.62 (3.6); N, 6.28 (5.9). IR (nujol): 1609 (w), 1364 (m), 1227 (m), 1070 (s), 1026 (m), 785 (s), 669 (m) $cm^{-1}$.

**[Zn(1−H)Br]$_\infty$.** A solution of **1** (50 mg, 0.41 mmol) in MeOH (2 mL) was combined with $ZnBr_2$ (22.8 mg, 0.10 mmol) to give a colorless solution. The mixture was stood at room temperature overnight to give colorless crystals, which were filtered off, washed with MeOH, and air-dried. Yield: 8.6 mg (32%). Anal. Calcd (Found) for $C_7H_8BrNOZn$: C, 31.43 (31.7); H, 3.01 (3.0); N, 5.24 (5.2). IR (nujol): 2361 (m), 1608 (s), 1580 (s), 1226 (m), 1166 (s), 1136 (m, br), 1066 (s), 1025 (m), 781 (s), 722 (m) $cm^{-1}$.

**[$Mn_4$(1−H)$_6Cl_4$].** $MnCl_2$·$4H_2O$ (70.1 mg, 0.354 mmol) was combined with **1** (87.2 mg, 0.708 mmol) in MeOH (0.75 mL). Very dark red triangular prisms formed after several weeks at 4 °C. X-ray crystallography showed that the known complex [$Mn_4$(**1**−H)$_6Cl_4$] had formed.

**[$Ni_4$(1−H)$_4Cl_4$(MeOH)$_4$]/[$Ni_4$(1−H)$_4Cl_4$($H_2O$)$_4$]·$H_2O$. 1** (54.0 mg, 0.44 mmol) was combined with $NiCl_2$·$6H_2O$ (104 mg, 0.44 mmol) in MeOH (1 mL) to give a green solution that was stood overnight at 20 °C. A green crystalline solid formed, which was filtered off and washed with a small amount of cold MeOH. X-ray crystallography of a single crystal selected from this batch showed [$Ni_4$(**1**−H)$_4Cl_4$(MeOH)$_4$], but microanalysis indicated that drying of the compound in an oven at 40 °C leads to the replacement of the MeOH ligands by $H_2O$ to give [$Ni_4$(**1**−H)$_4Cl_4$($H_2O$)$_4$]·$H_2O$ (see text). Yield: 94 mg (89%). Anal. Calcd (Found) for [$Ni_4$(**1**−H)$_4$-$Cl_4$($H_2O$)$_4$]·$H_2O$: C, 35.21 (35.0); N, 5.87 (5.8); H, 4.43 (4.7). IR (KBr disc): 3600−3192 (br), 2921 (m), 2851 (m), 2135 (w), 1607 (s), 1578 (m), 1465 (s), 1446 (s) 1384 (m), 1364(m), 1272 (w), 1246 (w), 1220 (w), 1164 (m), 1107 (m), 1075 (s), 1015 (m), 934 (w), 893 (w), 781 (s), 746 (m), 780 (m) 653 (s), 560 (m), 535 (m), 502 (m) $cm^{-1}$.

**[$Ni_4$(1−H)$_4Cl_2$(OAc)$_2$(MeOH)$_2$]. 1** (156 mg, 1.28 mmol) was dissolved in MeOH (3 mL), and a solution of $NiCl_2$·$6H_2O$ (151 mg, 0.64 mmol) and Ni(OAc)$_2$·$4H_2O$ (156 mg, 0.64 mmol) in MeOH (3 mL) was added. The resulting green solution was evaporated slowly at 20 °C to give a green crystalline solid, which was filtered off, washed with $Et_2O$, and air-dried. Yield: 213 mg (64%). Anal. Calcd (Found) for [$Ni_4$(**1**-H)$_4Cl_2$(OAc)$_2$(MeOH)$_2$]·$4H_2O$ ($C_{34}H_{54}Cl_2N_4Ni_4O_{14}$): C, 38.95 (38.4); H, 5.19 (4.8); N, 5.34 (5.4). IR (KBr disc): 3270.1 (s, br), 2922 (m), 2851 (m), 1655 (m), 1606 (s), 1579 (s), 1556 (s), 1463 (s), 1451 (s), 1414 (s) 1358 (m), 1272 (w), 1244 (w), 1219 (w), 1163 (m) 1111 (m), 1079 (s), 1015 (m), 929 (w), 894 (w) $cm^{-1}$.

**X-ray Crystallography.** The X-ray crystallographic results are summarized below. Structures were solved by direct methods, and refined against $|F|^2$ using anisotropic thermal displacement parameters for all non-hydrogen atoms. Hydrogen atoms were placed in calculated positions and refined using a riding model (except where noted below). Thermal ellipsoid plots of all structures are given in the Supporting Information.

**Crystal Data. [$Cu_2$(1)$_2$(1−H)$_2Cl_2$]·$CH_3OH$.** $C_{29}H_{38}Cl_2Cu_2N_4O_5$. Monoclinic, $P2_1/c$, $a$ = 13.4562(16) Å, $b$= 14.3942(17) Å, $c$ = 15.9350(19) Å, $V$ = 3086.4(6) Å$^3$, $\beta$ = 90.273(2)°, $Z$ = 4, $D_{calc}$ = 1.55 g $cm^{-3}$. This structure was refined as a pseudo-merohedral twin with a 24% contribution from a second domain, with 19 043 reflections measured of which 7073 were unique ($R_{int}$ = 0.063). The hydrogen atoms involved in the hydrogen bond between monomers were found on the electron density difference map. The final $R$ factor for 4973 observed reflections ($I > 2\sigma(I)$) with 393 variables was 0.071 ($R_w$ = 0.146). Residual electron density peaks: max = 0.78, min = −0.88 e·Å$^{-3}$.

**[$Cu_2$(1)$_2$(1−H)$_2Br_2$]·$H_2O$.** $C_{28}H_{36}Br_2Cu_2N_4O_5$. Monoclinic, $P2_1/c$, $a$ = 13.606(2) Å, $b$ = 14.407(3) Å, $c$ = 15.591(3) Å, $V$ = 3056.2(9) Å$^3$, $\beta$ = 90.107(3)°, $Z$ = 4, $D_{calc}$ = 1.73 g $cm^{-3}$, with 13 642 reflections measured of which 4369 were unique ($R_{int}$ = 0.088). This structure was refined as a pseudo-merohedral twin with a 39% contribution from a second domain. The hydrogen atoms involved in the hydrogen bond between monomers were found on the electron density difference map; however, the H atoms of the $H_2O$ solvent molecule were not located. The final $R$ factor for 1739 observed reflections ($I > 2\sigma(I)$) with 375 variables was 0.041 ($R_w$ = 0.072). The quality of the dataset precluded an ideal data/parameter ratio; however, it may be noted that the $R$ factor based on *all* 4369 data was 0.1271. Residual electron density peaks: max = 1.16, min = −0.42 e·Å$^{-3}$.

**[$Cu_2$(1)$_2$(1−H)$_2$]($ClO_4$)$_2$.** $C_{28}H_{34}Cl_2Cu_2N_4O_{12}$. Monoclinic, $P2_1/c$, $a$ = 10.0579(6) Å, $b$ = 11.7112(7) Å, $c$ = 13.7986(8) Å, $V$ = 1568.02(16) Å$^3$, $\beta$ = 105.2620(10)°, $Z$ = 4, $D_{calc}$ = 1.60 g $cm^{-3}$, with 9572 reflections measured of which 3603 were unique ($R_{int}$ = 0.028). The final $R$ factor for 3149 observed reflections ($I > 2\sigma(I)$) with 223 variables was 0.041 ($R_w$ = 0.10). Residual electron density peaks: max = 1.76 (0.76 Å from Cu), min = −0.68 e·Å$^{-3}$.

**[$Cu$(2)$_2$Cl]Cl·$H_2O$.** $C_{16}H_{24}Cl_2CuN_2O_3$. Monoclinic, $P2_1$, $a$ = 9.1495(8) Å, $b$ = 8.6211(7) Å, $c$ = 12.9070(11) Å, $\beta$ = 97.6750-(10)°, $V$ = 1008.97(15) Å$^3$, $Z$ = 4, $D_{calc}$ = 1.74 g $cm^{-3}$, with 5197 reflections measured of which 1938 were unique ($R_{int}$ = 0.030). The H atoms of the alcohol groups of the ligand and of the $H_2O$ molecule were found on the electron density difference map. The final $R$ factor for 3026 observed reflections ($I > 2\sigma(I)$) with 237 variables was 0.026 ($R_w$ = 0.054). Flack parameter = 0.015(9). Residual electron density peaks: max = 0.50, min = −0.21 e·Å$^{-3}$.

**[$Cu_2$(2)$_3$(2−H)$Br_2$]Br·2($H_2O$).** $C_{32}H_{47}Br_3Cu_2N_4O_6$. Monoclinic $P2_1$, $a$ = 10.5843(3) Å, $b$ = 16.3320(4) Å, $c$ = 11.9571(3), $\beta$ = 115.037(1) °, $V$ = 182.72(8), $Z$ = 4, $D_{calc}$ = 1.68 g $cm^{-3}$, with 33 306 reflections measured of which 10 494 were unique ($R_{int}$ = 0.041). The H atoms of the included $H_2O$ molecules could not be located. The final $R$ factor for 9402 observed reflections ($I > 2\sigma$-($I$)) with 440 variables was 0.029 ($R_w$ = 0.071). Flack parameter = 0.024(6). Residual electron density peaks: max = 0.95, min = −0.52 e·Å$^{-3}$.

**[Zn(1−H)Cl]$_\infty$.** $C_7H_8ClNOZn$. Orthorhombic, $P2_12_12_1$, $a$ = 5.0670(6) Å, $b$ = 9.1795(10) Å, $c$ = 18.293(2) Å, $V$ = 850.83(17) Å$^3$, $Z$ = 2, $D_{calc}$ 1.41 g $cm^{-3}$, with 6093 reflections measured of

which 3286 were unique ($R_{int}$ = 0.023). This structure was refined as a racemic twin with an equal contribution from the two domains. The final *R* factor for 1832 observed reflections ($I > 2\sigma(I)$) with 102 variables was 0.031 ($R_w$ = 0.074). Residual electron density peaks: max = 2.17 (1.32 Å from Zn), min = −0.28 e·Å$^{-3}$.

**[Ni$_4$(1−H)$_4$Cl$_4$(MeOH)$_4$].** $C_{32}H_{48}Cl_4N_4Ni_4O_8$. Monoclinic, *C*2/*c*, *a* =16.2641(7) Å, *b* = 15.0302(7) Å, *c* = 16.6497(11) Å, $\beta$ = 100.9830(10)°, *V* = 3995.5(4) Å$^3$, *Z*′ = 4, $D_{calc}$ = 1.645 g cm$^{-3}$, with 12 349 reflections measured of which 4620 were unique ($R_{int}$ = 0.024). The final *R* factor for 4023 observed reflections ($I > 2\sigma(I)$) with 247 variables was 0.046 ($R_w$ = 0.128). Residual electron density peaks: max = 1.50 (1.16 Å from N31), min = −0.49 e·Å$^{-3}$.

**[Ni$_4$(1−H)$_4$Cl$_2$(OAc)$_2$(MeOH)$_2$]·0.5(CH$_3$OH).** $C_{69}H_{96}Cl_4N_8Ni_8O_{21}$. Orthorhombic, *Pca*2$_1$, *a* = 15.9492(13) Å, *b* = 35.895(3) Å, *c* = 13.9089(11) Å, *V* = 7962.8(11) Å$^3$, $D_{calc}$ = 1.683 g cm$^{-3}$, with 49 334 reflections measured of which 18 174 were unique ($R_{int}$ = 0.044). The ADDSYM routine Platon[35] suggested missed symmetry elements and that the space group was *Pbca*; however, refinement in *Pca*2$_1$ as a racemic twin (with a 3:1 contribution from the two domains) produced a far more satisfactory result. Residual electron density (55 electrons per unit cell) corresponding to further solvate molecules could not be modeled satisfactorily and was accounted for with the SQUEEZE routine in Platon. The H atoms of the alcohol groups of the coordinated $CH_3OH$ ligands, as well as of the guest $CH_3OH$ molecule, could not be located. The final *R* factor for 14121 observed reflections ($I > 2\sigma(I)$) with 1002 variables was 0.058 ($R_w$ = 0.132). Residual electron density peaks: max = 1.64; min = −0.73 e·Å$^{-3}$.

(35) Spek, A. L. *PLATON, A Multipurpose Crystallographic Tool*; Utrecht University: Utrecht, The Netherlands, 2001.

**Acknowledgment.** We thank Prof. Geoffrey B. Jameson for assistance in refining the crystal structures of [Cu$_2$(**1**)$_2$(**1**−H)$_2$Cl$_2$] and [Cu$_2$(**1**)$_2$(**1**−H)$_2$Br$_2$]. We are grateful to the following funding agencies for financial support: the Japan Society for the Promotion of Science, the Japan Science and Technology Agency (ERATO fund), the Massey University Research Fund, the RSNZ Marsden Fund, and NSERC of Canada.

**Supporting Information Available:** Crystallographic data in CIF format, crystallographic figures, and additional magnetic susceptibility data. This material is available free of charge via the Internet at http://pubs.acs.org.

IC701757E